Food Research International 222 (2025) 117757

Contents lists available at ScienceDirect

Food Research International

journal homepage: www.elsevier.com/locate/foodres

Unveiling the survivability of probiotic CA15 strain with and without fluconazole co-administration and its effect on gut microbiota and metabolome through SHIME® model

Amanda Vaccalluzzo [a], Giuseppe Celano [b,*], Francesco Maria Calabrese [b], Alessandra Pino [a,c], Cinzia Caggia [a,c], Maria De Angelis [b], Cinzia Lucia Randazzo [a,c,*]

[a] Department of Agriculture, Food and Environment, University of Catania, Italy
[b] Department of Soil, Plant and Food Science, University of Bari Aldo Moro, Italy
[c] ProBioEtna srl, Spin off of the University of Catania, Catania, Italy

ARTICLE INFO

Keywords:
Upper GIT
Fed and fasted conditions
RT-qPCR
SCFAs and BCFAs
VOCs
meta-taxonomic

ABSTRACT

The aim of the present study was to investigate the survival and functional impact of the probiotic *Lacticaseibacillus rhamnosus* CA15 strain on gut microbiota and metabolome, under simulated gastrointestinal conditions, through the SHIME® model. The experimental design included both fed and fasted conditions, and co-administration of fluconazole. A colonic incubation of up to 24 h was carried out, and CA15 availability was assessed using strain-specific RT-qPCR. In addition, the effects of the CA15 strain on metabolome and microbiota profiles were explored. Results showed that the fasted condition did not negatively affect the survival of the CA15 strain on the ileal stage. Moreover, fluconazole co-administration did not interfere with strain survivability. Meta-taxonomic 16S rRNA and metabolome profiles of the colonic fraction revealed significant variation in both microbial composition and metabolic compounds. Fluconazole determined a reduction of *Firmicutes* and an increase of *Proteobacteria*. In particular, a decrease of *Dorea*, *Mitsuokella*, *Lactobacillus*, *Oscillospiraceae* UCG-002, and *Bifidobacterium* genera, as well as *Christensenellaceae*_R-7_group and *Eubacterium hallii*. The co-administration of the CA15 strain, in the colonic fraction, counteracted the changes induces by the antimycotic treatment. Furthermore, CA15 administration significantly increased volatile organic compounds, short- and branched-chain fatty acids, particularly heptanoic, acetic, propanoic, and isobutyric acids. In conclusion, the CA15 stain demonstrated good survivability and a positive modulation of the gut microbiota and metabolome, supporting its potential as a functional probiotic. The use of the dynamic SHIME® model provided valuable insights into the delivery and performance of the probiotic CA15 strain on the GIT, under both fed and fasted conditions.

1. Introduction

In recent years, there has been an increase in knowledge of the health benefits associated with probiotic intake. The efficacy of probiotics has been demonstrated by scientific evidence based on both *in vitro* and *in vivo* studies. The beneficial effects of probiotics are influenced by both the dose and the minimum recommended intake. In particular, the cell density of probiotics should be 10^9 CFU/mL or CFU/g (Wendel, 2022). According to FAO/WHO (2002), who defined 'probiotics' as *'live microorganisms that, when administered in adequate amounts, confer a health benefit to the host'*, it is important that a probiotic product contains an adequate number of viable microorganisms capable of replicating in the gastrointestinal tract (GIT) environment, colonising the gut microbiota. For this reason, probiotics must be able to tolerate exposure to various stressors during their lifecycle, including production, storage and passage through the human body, where acidic conditions, bile, and gastric and pancreatic enzymes can impact their survival (Wendel, 2022).

Adequate intake of viable probiotics is a necessary condition to ensure human health and well-being, so oral administration of encapsulated probiotics is a potential solution to this problem (Han et al.,

* Corresponding authors.
E-mail addresses: amanda.vaccalluzzo@unict.it (A. Vaccalluzzo), giuseppe.celano@uniba.it (G. Celano), francesco.calabrese@uniba.it (F.M. Calabrese), alessandra.pino@unict.it (A. Pino), ccaggia@unict.it (C. Caggia), maria.deangelis@uniba.it (M. De Angelis), cinzia.randazzo@unict.it (C.L. Randazzo).

https://doi.org/10.1016/j.foodres.2025.117757
Received 9 April 2025; Received in revised form 15 July 2025; Accepted 25 October 2025
Available online 31 October 2025

2024). Over the years, oral delivery systems (ODS) based on polysaccharides such as, starch, cellulose, chitosan, and their derivatives have been developed to form a protective layer for probiotics, as well as encapsulation technologies that mainly include emulsion cross-linking, atomization, freeze-dried, and others, to preserve the bioavailability of probiotics (Wang et al., 2025; Yang, Qiao, et al., 2024). To maximize the *ex vivo* stability of probiotics, encapsulation is a helpful biotechnological tool that preserve the longevity and functionality of probiotics. These techniques are developed to protect probiotics during their shelf-life, ensuring their viability so that they can quickly become active once they reach the GIT (Wang et al., 2025).

The upper GIT presents several challenges for probiotic delivery; indeed, after the passage from the oesophagus, probiotics reach the stomach, where they are exposed to the acidic gastric juice, that could be extremely detrimental to bacteria cells and compromising their viability (Wendel, 2022). In addition, other adverse conditions present in the stomach including ionic strength, enzyme activities (*e.g.* pepsin and lecithin) and mechanical churning can negatively affect the viability of probiotics (Han et al., 2024; Wang et al., 2025). The time of exposure to stomach harsh condition could vary from 5 min to 2 h, depending on fasting or fed conditions (Minelli & Benini, 2008). Moreover, conditions in the small intestine, particularly the presence of bile acids and enzymes like trypsin and chymotrypsin, can further reduce cell density, thereby compromising the survival of probiotic strains (Yang, Wei, et al., 2024; Wendel, 2022). Although pH values and the availability of macronutrients increase in the colon, probiotic bacteria encounter a hostile environment, characterized by colonization resistance and intense competition for nutrients from the commensal microbiota (Hoek & Merks, 2017; Rinninella et al., 2019).

Furthermore, the oral administration of antimicrobial agents, such as antibiotic, in addition to the harsh conditions of the GI tract, can significantly impacts the probiotics survivability (Han et al., 2021). The mechanism of action of many antibiotics and/or antimycotics, including triazoles such as fluconazole, is still unclear, as they may have direct antimicrobial activity against both selected bacterial pathogens and gut commensals (Dornelas-Figueira et al., 2023). Fluconazole, for instance, is widely described as an antifungal drug from the bis-triazole class, manly used for treatment and prophylaxis of localised and systemic *Candida spp.* infections (Pappas et al., 2016). It is able to inhibit fungal ergosterol synthesis by targeting lanosterol 14α-demethylase and is generally dosed in a range of 150 mg to 800 mg/day in more severe fungal infections (U.S. Food and Drug Administration FDA, 2022). Moreover, due to its metabolic stability, which avoids possible alterations caused by food intake and gastric acidity, fluconazole is rapidly absorbed into the bloodstream, enhancing its therapeutic effect (Heng et al., 2021; Martin, 1999). Recent studies have found that fluconazole exposure may indirectly influence the gut microbiota, possibly reducing the abundance of certain commensal species, despite its primary antifungal mechanism. In addition, evidence suggests that this antifungal drug may interfere with beneficial microbes through non-target mechanisms, altering intestinal homeostasis (Heng et al., 2021). However, the combined use of fluconazole with specific probiotic strains leads to higher rates of mycological healing and reduced symptom recurrence than antimycotic treatment alone, suggesting a synergistic effect between antimycotic treatment and probiotic supplementation (Martinez et al., 2009; Vahedpoor et al., 2021). In this regard, the survival rate of probiotic after exposure to pancreatic and gastric juices or eventually administration of antibiotic treatment can vary significantly, sometimes by several log units, depending on formulation, lyophilisation and storage conditions, affecting probiotic products. Indeed, the number of viable microorganisms needed to achieve a clinical effect is generally considered to be 10^6 CFU/mL in the small intestine and 10^8 CFU/g in the colon (Minelli & Benini, 2008).

In recent years, numerous *in vitro* digestion models, static or dynamic, single or multi-compartmental, have been developed and widely used as an alternative tool to study the digestion of food or encapsulated probiotic ever closer to the human GIT (Li et al., 2020). The application of static *in vitro* models often oversimplifies digestive processes, so they are mainly used for mechanistic studies and hypothesis building. This limitation has been overcome by dynamic *in vitro* models, allowing the simulation of the dynamic aspects of digestion, such as digesta transport, continuous secretions of gastric and pancreatic juice, varying enzyme concentrations and controlled pH changes over time, that occur under *in vivo* conditions. One of the most representative dynamic models is the Human Intestinal Microbial Ecosystem Simulator (SHIME®), developed by Molly et al. (1993) and owned by ProDigest and the University of Ghent (Belgium). According to Van de Wiele et al. (2015), the SHIME® is one of the few gut models that reproduces the entire gastrointestinal tract, including the acidic environment in the stomach and exposure to bile salts in the small intestine up to the simulation of the colon, providing insights into food digestion and associated changes in the human gut microbiota. SHIME® is recognized for its ability to simulate the bioavailability and influence of probiotics in the gastrointestinal tract, allowing for easier reproducibility of data and reduction of variations resulting from the *in vivo* model. Furthermore, due to the invasive investigation of intestinal phases, they can provide mechanistic insight into the effects of probiotics, allowing end-point measurements at all stages of digestion (Marzorati, 2018).

The aim of the present work was to evaluate the survivability of the probiotic *Lacticaseibacillus rhamnosus* CA15 (DSM 33960) using upper GIT SHIME® model. Specifically, the simulation passage through the stomach and upper intestinal tract under both fasted and fed conditions was investigated. In addition, the simultaneous administration of the antimycotic fluconazole (200 mg) under fasted conditions and its effect on the colonic fraction after 24 h of incubation were also investigated.

2. Materials and methods

2.1. Capsules preparation

The L. *rhamnosus* CA15 (DSM 33960) strain belonging to the ProBioEtna srl culture collection was previously *in vitro* characterized for probiotic properties, including functional (antagonistic activity against pathogens, organic acid and lactic acid production, antioxidant and anti-inflammatory activities, adhesion to intestinal mucus CaCo-2 and VK7/E6E7 cell lines, etc) and safety characteristics (haemolytic, DNase, and gelatinase activities, mucin degradation, production of biogenic amines, and resistance to antimicrobials) (Pino et al., 2022). The probiotic strain was freeze-dried and subjected to encapsulation using the MS-4/7 and MS-6/N ModelS Capsule Machine (MultiPharma, Italy). Each capsule, made by SYNBIOTEC srl (Camerino, Italy), contained 10 billion of the CA15 strain, corn-starch (100 mg) as bulking agent, and vegetable transparent capsule (60 mg) of size 2 made of Hypromellose. A placebo capsule (corn-starch and vegetable transparent capsule, without probiotic strain) was used as control.

2.2. Survivability of the L. rhamnosus CA15 strain during the upper GIT digestion under fasted and fed conditions

The survivability of the probiotic L. *rhamnosus* CA15 strain during the upper GIT digestion, was evaluated through the SHIME® system under both fasted and fed conditions (Fig. 1), following the protocols proposed by Marzorati and co-workers (2021) and Jannin et al. (2023). In detail, a double-jacketed reactor, maintained at 37 °C under constant stirring (300 rpm), was used to simulate both the stomach and small intestine digestions. The encapsulated CA15 strain was placed inside the reactor using a capsule sinker. To mimic the mechanical stress occurring during the *in vivo* digestion, the capsule sinker was placed in the middle of the liquid, perpendicularly to the direction of the agitation. A control reactor, without capsule, was included in all the assays as background medium. To simulate both fasted and fed conditions, the pH profile, enzyme levels, and retention times were set up according to the protocol

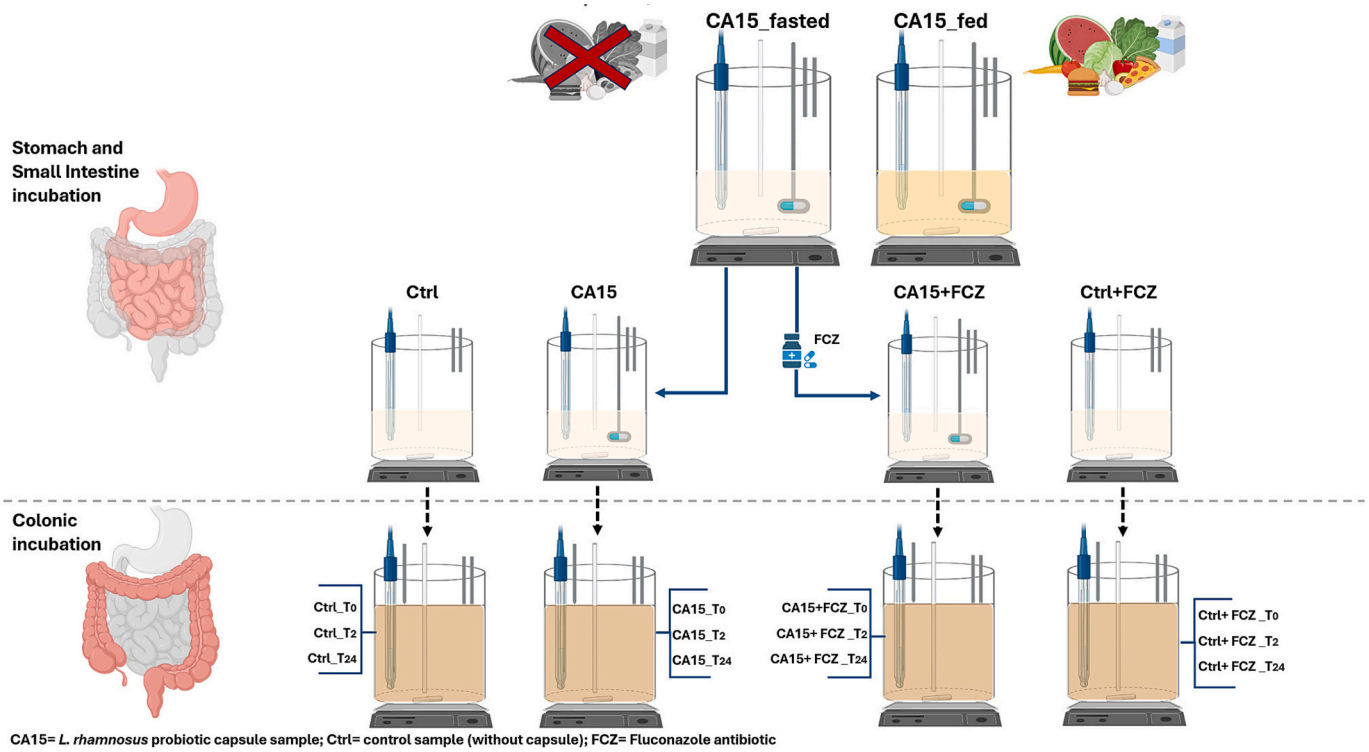

Fig. 1. Schematic representation of the study design. In detail, during stomach/small intestinal digestion, capsules of the probiotic L. *rhamnosus* CA15 were subjected to FED and FASTED conditions using the SHIME® upper-GIT system. Subsequently, under FASTED conditions, capsule survival was tested with and without fluconazole co-administration. Following these conditions, colonic incubation maintained for 24 h was mimicked.

reported by Marzorati and co-workers (2021). Specifically, under fasted condition, a gastric solution (76 mL at pH 2.0), containing KCl 0.66 g/L, NaCl 3.63 g/L, mucin 3.95 g/L, 0.4 mL of lecithin (GmbH + Co. KG, Germany) (3.4 g/L), and 3.6 mL pepsin (Sigma Aldrich, Italy) (10 g/L) was used to simulate the stomach digestion and maintained for 45 min of incubation. Subsequently, a 35.2 mL of pancreatic juice ($NaHCO_3$ 2.6 g/L, Oxgall 4.8 g/L and pancreatin 1.9 g/L), 2.15 mL trypsin (GmbH + Co. KG, Germany) (10 g/L) and 2.7 mL chymotrypsin (GmbH + Co. KG, Germany) (10 g/L) were added. The pH of the small intestine was gradually increased from 2.0 to 6.5 and maintained at this pH over 27 min to simulate the duodenal fraction, followed by jejunal (pH up to 7.5 maintained for 63 min) and ileal (constant pH 7.5 for 90 min) fractions. An increase in pH was achieved by the addition of $NaHCO_3$ (8.4 g/L) at 60, 90 and 120 min, mimicking the dilution of the intestinal contents.

Under fed condition, a gastric solution (76 mL), containing SHIME® nutritional medium (PDNM001B 20.53 g/L, ProDigest, Ghent, Belgium), NaCl (3.63 g/L), KCl (0.65 g/L), 0.4 mL lecithin (13.5 g/L), and 3.6 mL pepsin (40 g/L) at pH 4.6 was added to the vessel and maintained for 120 min with a sigmoidal pH decrease from 4.6 to 2. After incubation in the stomach, a small intestine phase, comprising duodenum, jejunum, and ileum, was performed as described above, with different pancreatic juice compositions ($NaHCO_3$ 7.7 g/L, Oxgall 15 g/L and pancreatin 10 g/L, added with 2.15 mL trypsin 10 g/L and 2.7 mL chymotrypsin 10 g/L). To simulate intestinal dilution, an increase in pH was achieved by the addition of $NaHCO_3$ (4.8 g/L) at 60, 90 and 120 min of intestinal incubation. The increase and decrease in pH were automatically controlled, by pH-meter probe (ProSense, Oosterhout, The Netherlands), and adjusted by the dosage of HCl (0.5 M) and NaOH (0.5 M). A reactor with a placebo capsule was used as a control sample in both fasted and fed conditions. All the SHIME® assays were performed in duplicate.

Samples were collected from both the stomach and small intestine fractions (duodenum, jejunum and ileum) and subjected to culture-dependent analysis. Briefly, samples were serially diluted using the anaerobic PBS, containing 8.8 g/L of K_2HPO_4, 6.4 g/L of KH_2PO_4, 8.5 g/L of NaCl, and 0.5 g/L of L-cysteine HCl, then cultured on Lactobacilli MRS Agar medium (BD Difco™, Italy) and incubated under anaerobic conditions at 37 °C for 48 h.

All the used reagents were purchased by Sigma-Aldrich (Milan, Italy). The plate count assay was performed in triplicate and results were reported as mean log CFU/mL and standard deviation.

2.3. Survivability of the L. rhamnosus CA15 strain during the upper GIT digestion under fasted condition and in presence of fluconazole

The survivability of the probiotic L. *rhamnosus* CA15 strain through the upper GIT SHIME® model in presence of the antimycotic fluconazole was further evaluated under fasted condition (Fig. 1), following the protocol previously mentioned (Marzorati et al., 2021) In detail, the gastric digestion was initiated with the simultaneous addition of the encapsulated CA15 strain and fluconazole (200 mg). Specifically, the encapsulated CA15 strain was placed inside the reactor in a capsule sink and the fluconazole, dissolved in distilled water, was directly injected through an additional port of the SHIME® reactor. Reactors with a placebo capsule with and without the fluconazole addition were used as control samples. All the SHIME® assays were performed in duplicate.

The survivability of the CA15 strain was evaluated by culture dependent method, as previously described, and the results were reported as mean log CFU/mL and standard deviation of three replicates.

2.4. Simulation of the colonic incubation

Following the upper GIT digestion (Fig. 1), a colonic incubation, under fasted condition, with and without the fluconazole, was simulated for 24 h, according to the protocol proposed by Marzorati and co-workers (2021). A stool sample, obtained from a healthy volunteer (female, 50 y), was provided by Department of General Surgery and Medical Surgical Specialties, AOU Policlinico G. Rodolico-San Marco Hospital, Catania (Italy), according to the protocol study approved the

local Ethical Committee (registration number 163/2022/PO). The stool sample was previously evaluated for microbial composition (Rinninella et al., 2019), and opportunely treated as reported by Van den Abbeele et al. (2018). In detail, a 1:10 (*w/v*) mixture of faecal sample and anaerobic phosphate buffer (K_2HPO_4 8.8 g/L; KH_2PO_4 6.8 g/L; sodium thioglycolate 0.1 g/L; sodium dithionite 0.015 g/L) was homogenised for 10 min (BagMixer 400, Interscience, Louvain-LaNeuve, Belgium), the mixture was centrifuged (2 min, 500 *g*) and the large particles removed. The faecal slurry obtained (20 % *v*/v) was added to 160 mL fresh colonic anaerobic medium [KH_2PO_4 (6.6 g/L), K_2HPO_4 (20.5 g/L), NaCl (5 g/L), yeast extract (2 g/L), peptone (2 g/L), glucose (1 g/L), starch (2 g/L), mucin (1 g/L), L-cysteine HCl (0.5 g/L), Tween® 80 (2 mL)], 40 mL of anaerobic PBS [K_2HPO_4 (8.8 g/L), KH_2PO_4 (6.4 g/L), NaCl (8.5 g/L) and L-cysteine HCl (0.5 g/L)]. The colonic incubation was carried out under anaerobic conditions at 37 °C, and 90 rpm agitation. A fixed pH interval between 6.5 and 5.8 was implemented and automatically adjusted. The colonic incubation was performed in duplicate, following previous small intestine digestion. Samples for metagenetic and metabolomic analyses were collected after 0, 2, and 24 h of incubation.

2.5. Design and validation of strain-specific primers

In order to specifically detect the L. *rhamnosus* CA15 strain in samples collected from the colonic fraction, the strain-specific primer pair CA15_F3 (AAACGCTCCCAGCACACC) and CA15_R1 (ATCCCCGTCATGCTGATG) was designed on the unique region of the whole genome, identified through the study of the phylogenetic relationships between the CA15 strain and 202 *L. rhamnosus* strains genomes available in the NCBI Assembly database at the time of the study. The variable region, used to design the strain-specific primers was submitted to the BankIt (BankIt2979291 CA15_contig0002_344127–342571), under the GenBank accession number PV931795. All details of the designed primer pair can be found in Supplementary Table 1. The specificity of the CA15_F3 and CA15_R1 primers was firstly validated by conventional PCR against twenty strains, isolated by vaginal swabs, belonging to the L. *rhamnosus* species and other phylogenetically close and unrelated species ascribed to *Lacticaseibacillus paracasei*, *Lacticaseibacillus casei*, *Lactiplantibacillus plantarum*, *Lactobacillus jensenii*, and *Lactobacillus johnsonii*. In detail, total genomic DNA was isolated from each strain by using the PureLink™ Genomic DNA Mini Kit (Thermo Fisher Scientific) and subjected to PCR amplification as follow. The PCR reaction was performed in a final volume of 25 μL using the 2× YourTaq™ PCR Master Mix (BiotechRabbit, Berlin Germany) and following the manufacturer's instructions. The PCR cycling conditions were set as follows: 94 °C for 2 min, followed by 95 °C for 30 s, 64 °C for 20 s and 72 °C for 30 s for 30 cycles and then 72 °C for 5 min. Agarose gel (2 %) electrophoresis was conducted at 80 V to validate the PCR products. The specificity and amplification efficiency (E) of the designed primer pair were also verified by qPCR, using a 10× dilution of the DNA of the L. *rhamnosus* CA15 strain as a reference standard. The qPCR reaction was performed using the QuantiNova™ SYBR Green PCR Kit (Qiagen). Cycling conditions consisted of a holding phase at 94 °C for 2 min, followed by 35 cycles at 95 °C for 30 s, 64 °C for 20 s and 72 °C for 30 s. The melting range was set between 75 °C and 95 °C. The slope of the regression curve between the logical values of the DNA concentrations and the mean values of the cycle threshold (Ct) was used to calculate the primer efficiency using the equation: $E = 0.5\,(10(-1/\text{slope})) \times 100$. The qPCR reaction was performed with a Rotor Gene Q instrument (Qiagen, Milan, Italy). Each reaction was repeated at least three times.

2.6. Survivability of the L. rhamnosus CA15 strain in the colonic fraction

A strain-specific RT-qPCR assay was carried out to evaluate the survivability of the probiotic L. *rhamnosus* CA15 strain in the colonic fraction. In detail, lumen samples (1 mL) collected after 0, 2, and 24 h of incubation, were centrifuged at 20,000 x*g* for 10 min, washed with anaerobic PBS, and subjected to RNA extraction using the ZymoBIOMICS™ RNA Miniprep Kit (Zymo Research, Orange, CA, USA) according to the manufacturer's instructions. The concentration of the RNA template was checked using the Qubit™ 4 fluorometer (Thermo Fisher Scientific, San Jose, CA, USA). RNA templates were subjected to reverse transcription PCR (RT-PCR) analysis using the QuantiTect Reverse Transcription Kit (Qiagen, Hilden, Germany). The complementary DNA (cDNA) obtained was subjected to RT-qPCR using the previously reported primer pair and following the qPCR assay protocol detailed above. Each reaction was performed in triplicate.

2.7. gDNA extraction, meta-taxonomic analysis, and 16S bioinformatic analysis

Colonic lumen samples, collected after 24 h of incubation, were subjected to total genomic DNA isolation, following the protocol proposed by Lionetti and co-workers (2023). The V3-V4 region of the 16S rRNA gene was amplified by PCR as described by Klindworth et al. (2013) and Vaccalluzzo et al. (2022) and subjected to 16S rRNA gene sequencing using the Illumina MiSeq platform at the SYNBIOTEC srl (Camerino, Italy) facilities. Libraries for Illumina MiSeq sequencing were prepared as described by Lionetti et al. (2023). The raw data were deposited at the NCBI Sequence Read Archive (SRA) with the access code PRJNA1240936. Raw reads quality was checked by FastQC software. Denoising, quality filter, and taxonomic annotation were obtained using the QIIME2 microbiome platform (version 2020.8) and relative plugins locally installed into an *ad hoc* "anaconda" environment. In addition to the denoising phase, the QIIME q2-deblur plugin (https://github.com/qiime2/q2-deblur) was used for computing alpha (Shannon entropy and Faith's PD) and beta diversity metrics (Vaccalluzzo et al., 2022). The taxonomic assignment was obtained by using the database SILVA 138 (https://www.arb-silva.de/documentation/release-138/).

2.8. Analysis of volatile organic compounds of colonic fraction from SHIME®

Lumen samples obtained from the colonic fraction after 0, 2 and 24 h of incubation were analysed to determine the profile of volatile organic compounds (VOCs), Short Chain Fatty Acids (SCFAs), and Branched Chain Fatty Acids (BCFAs). To achieve a higher extraction efficiency, the procedure described by Lauriero et al. (2021), with slight modifications, was followed. Briefly, 1 g of sample added with 10 μL of 4-methyl-2-pentanol (9.9 μg/g final concentration) as internal standard (IS) was placed in a 10 mL glass vial and sealed with a polytetrafluoroethylene (PTFE)-coated silicone rubber septum. For the HD-SPME extraction method a divinylbenzene/Carboxen/polydimethylsiloxane (DVB-CAR-PDMS) fiber was exposed to the head-space for 40 min at 40 °C after 10 min of sample equilibration. The VOCs were thermally desorbed by transferring the fiber into the heated injection port (220 °C) of a Clarus 680 (Perkin Elmer, Beaconsfield, UK) gas chromatography equipped with an Rtx-WAX column (30 m × 0.25 mm i.d., 0.25 μm film thickness) (Restek Corporation, Bellefonte, PA, USA), and coupled to a Clarus SQ8MS (Perkin Elmer) (Vitellio et al., 2019). The temperature of source and transfer line were maintained at 250 and 230 °C, respectively. Peak identification analysis was performed on each chromatogram using the National Institute of Standards and Technology 2008 (NIST) library (Gaithersburg, MD, USA). VOCs identification used a peak area threshold of >1,000,000 and a match probability of 85 % or higher, followed by manual visual inspection of fragmentation patterns when required. The concentration of VOCs was expressed in μg/g of IS.

For the targeted analyses of SCFAs and BCFAs, a stock solution containing the mixture of SCFAs standards (acetic acid, butyric acid, propionic acid, isobutyric acid, methyl valerate and valeric acid) dissolved in ultrapure water was diluted to obtain a calibration curve

ranging from 1 μg·mL-1 to 250 μg·mL-1. Ten μl of 4-methyl-2-pentanol (final concentration of 1 mg/L) were added as internal standard in each dilution, before the analysis. We used the Total Ion Current (TIC) mode to obtain typical ions with a special mass-to-charge ratio of every SCFA and then used a Selective Ion Monitoring (SIM) mode to collect information of typical ions. Standard curve was made for each SCFA based on the data obtained by the SIM mode. The calibration curve was constructed by plotting the normalized peak area *versus* concentration of individual SCFAs. The relative peak of SCFAs in faecal sample was integrated and concentration (ppm) of SCFAs in faecal sample was calculated by the calibration curve equation. All tests were carried out in triplicate and values were reported as means ± SD of triplicates.

2.9. Statistical analysis

Data related to the survivability of the encapsulated probiotic L. *rhamnosus* CA15 strain in the upper GIT and colonic fraction, expressed as mean log CFU/mL and standard deviation and copies/μL log units, were subjected to One-way ANOVA followed by Tukey's *post hoc* test. Significant statistical differences were set as a $p < 0.05$. All statistical analyses, related to the survivability of the probiotic strain in the GIT, were performed using Statistica software (version 10.0 for Windows, TIBCO Software, Palo Alto, CA, USA). Alpha diversity was calculated using the Faith's Phylogenetic Diversity (PD) metric and visualized as interquartile boxplots. To assess statistically significant changes in both alpha and beta diversity, distance matrices based on Bray-Curtis, Jaccard, and Unweighted UniFrac were computed. VOCs data from untargeted analysis were compared by meaning of a non-parametric Wilcoxon rank-sum test ($p < 0.05$) combined with a fold change analysis (log2FC >2), statistically significant features have been graphically rendered as a Volcano plot by using EnhancedVolcano R-package in MeatboAnalystR-software (versione 2.0.0). Pairwise comparison of SCFAs (acetic acid, propanoic acid, isobutyric acid and butanoic acid) BCFA (isovaleric acid) was computed with Anova one-way corrected by Tukey's test.

3. Results

3.1. Survivability of the probiotic L. rhamnosus CA15 strain in the upper GIT under both fed and fasted conditions

Data on the survivability of the probiotic L. *rhamnosus* CA15 strain in the upper GIT, under both fasted and fed conditions, are shown in Fig. 2. Based on plate count, starting from an initial cell density of 10.60 log CFU/mL, the CA15 strain maintained, a cell density of about 6 log units, under fed condition. Specifically, a cell density of 6.27 log CFU/mL was registered during the gastric phase. In contrast, under fasted condition, the cell density of the strain was below the detection limit (< 1). During the digestion in the small intestine, the survival of the CA15 strain was revealed, under both treatments, in the three intestinal fractions. Under fed condition, no significant differences were observed in the duodenum and jejunum, with values of 6.70 and 6.79 log CFU/mL, respectively, while a significant reduction in the ileum, with a value of 6.03 log CFU/mL, was detected. Under fasted condition, no significant differences in viability were found across the small intestine fractions (from duodenum to ileum), with a slight increase in the jejunal (7.39 log CFU/mL) and ileal (7.35 log CFU/mL) phases, compared to duodenum (7.10 log CFU/mL). A comparison of the two conditions tested in the individual intestinal fractions showed significant differences in the jejunal and ileal phases, with greater survival under fasting condition (Fig. 2).

3.2. Survivability of the probiotic L. rhamnosus CA15 strain in the upper GIT under fasted condition and in presence of the antimycotic fluconazole

Based on the higher survivability obtained under fasted condition, the CA15 strain was tested in the upper GIT, both with and without the simultaneous addition of fluconazole (CA15 and CA15+ FCZ samples, respectively). As shown in Fig. 3, the L. *rhamnosus* CA15 strain showed the same trend both with and without the addition of the antimycotic, as reported above. In particular, the cell density of the strain in the stomach was below the detection limit (< 1), while in the small intestine fraction reached the value of 7.06 log CFU/mL.

3.3. Real-time qPCR for the detection of the L. rhamnosus CA15 strain in the colonic fraction

The cDNAs isolated from the colonic fraction, after 0, 2 and 24 h of incubation, were subjected to strain-specific real-time qPCR. The detection threshold revealed a coefficient of determination (R^2) and amplification efficiency (E) values of 98.6 % and 110 %, respectively. From the standard curves, the detection threshold ranged between 10.60 log CFU/mL and 2.60 log CFU/mL with Ct values of 4.04 and 28.66, respectively. Fig. 4 displays the detection data of the L. *rhamnosus* CA15

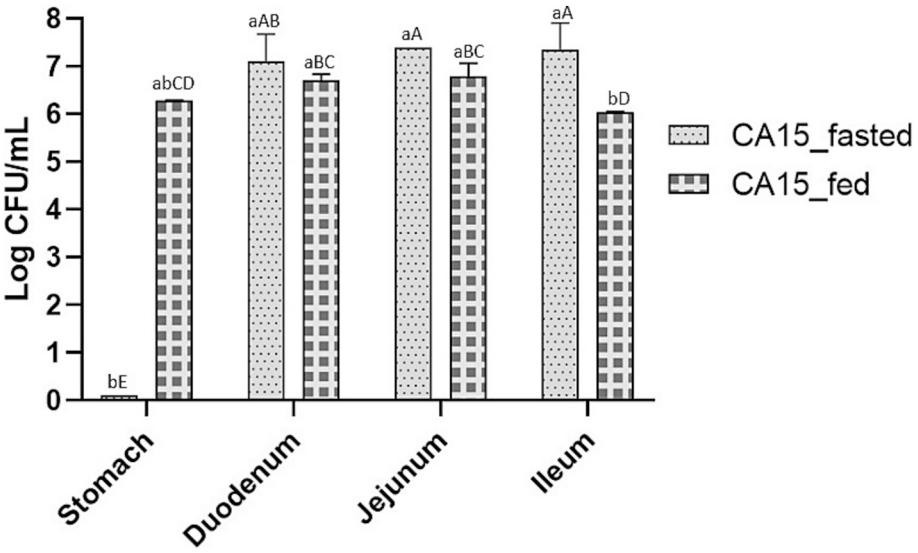

Fig. 2. Bar graph represents the survival of encapsulate probiotic L. *rhamnosus* CA15 after stomach and small intestine phases, under fed and fasted conditions. Data are expressed as CFU in log units ± standard deviation. [a–b]Different superscript letters within the same condition indicate significant differences at $p < 0.05$. [A–B]Different superscript letters within the same time of sampling indicate significant differences at $p < 0.05$.

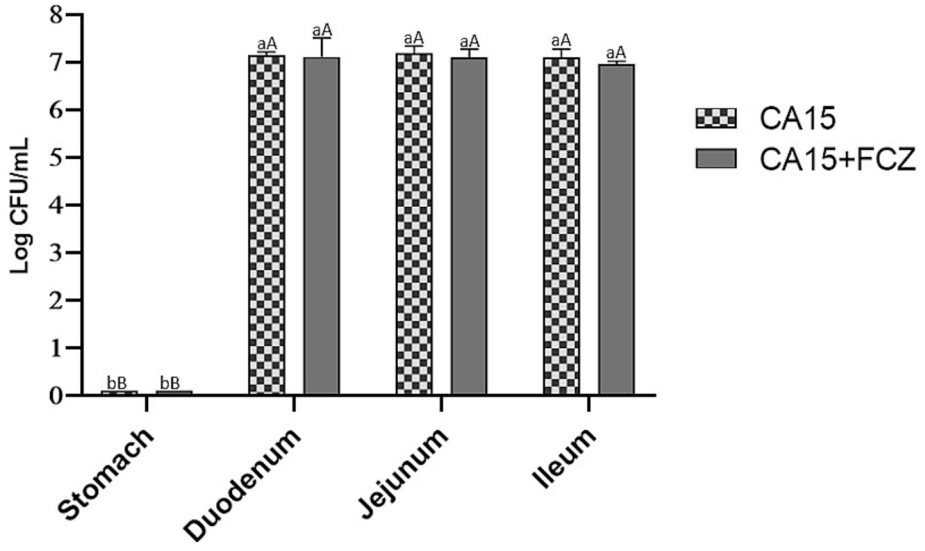

Fig. 3. Bar graph represents the survival of encapsulate probiotic *L. rhamnosus* CA15 after stomach and small intestine phases, under FASTED condition, with and without Fluconazole addition. Data are expressed as CFU in log units ± standard deviation. [a–b]Different superscript letters within the same condition indicate significant differences at $p < 0.05$. [A–B]Different superscript letters within the same time of sampling indicate significant differences at $p < 0.05$.

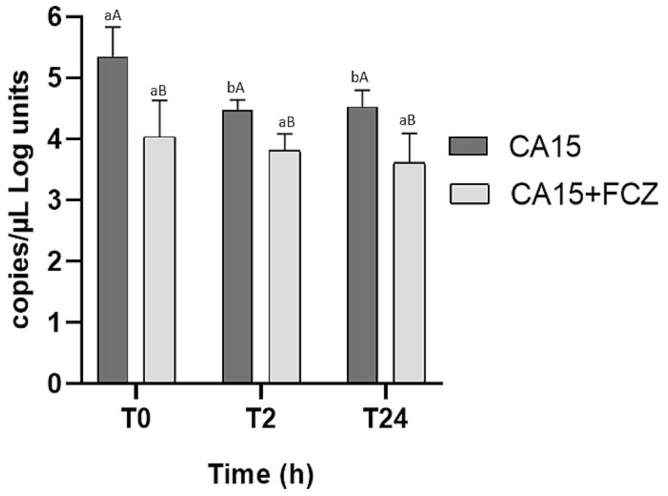

Fig. 4. Bar graph represents the detection of encapsulate probiotic L. *rhamnosus* CA15 during colonic incubation, under FASTED condition, with and without Fluconazole treatment. Data are expressed as copies/µL log units ± standard deviation. [a–b]Different superscript letters within the same condition indicate significant differences at $p < 0.05$. [A–B]Different superscript letters within the same time of sampling indicate significant differences at $p < 0.05$.

strain by real-time qPCR, expressed as copies/µL log units and standard deviation. Comparing treatments, significant differences emerged, at each sampling time, among samples with and without fluconazole (CA15 and CA15 + FCZ, respectively). Specifically, in the CA15 sample a value of 5.51 copies/µL log units was detected at T0, which decreased at T2 and T24, reaching values of 4.47 and 4.54 copies/µL log units, respectively. When CA15 strain was co-inoculated with fluconazole a value of 4.04 copies/µL log units was registered at T0, which decreased after 2 h and 24 h to values of 3.82 and 3.61 copies/µL log units, respectively. To verify the efficiency of the reactions with the strain-specific primers, cDNA extracted from control samples, both with and without fluconazole treatment, were subjected to real-time qPCR and no amplification copies were detected (data not shown).

3.4. 16S rRNA taxonomy profiles of the colonic fraction

Colonic fraction samples, collected at 24 h (T24) of incubation, were subjected to the sequencing of the V3 region of the 16S rRNA gene. The Faith's PD alpha diversity index, presented as a boxplot distribution in Supplementary Fig. S1, did not show significant differences in taxa distribution between CA15 with or without fluconazole, compared to the control. Beta diversity distances including Bray-Curtis, Jaccard, and Weighted and Unweighted UniFrac distances did not show divergent groups. The PCoA plot based on the unweighted UniFrac computed distances revealed no clustering (Supplementary Fig. S1b). In Fig. 5, the bar graph shows the most representative microbial genera, expressed as percentage values of relative frequency. Focusing on the microbial profiles, the *Escherichia coli-Shigella* genera were present with a relative frequency of 13.3 % and 15.63 % in the control (Ctrl) and CA15 samples (CA15), respectively, while they appeared reduced by the antimycotic treatment (CA15 + FCZ), reaching a value less than 1 %. It is interesting to highlight that the *Enterobacteriaceae* family was found lower in the CA15 (3.66 %) than in Ctrl (6.82 %) samples. Surprisingly, the fluconazole administration determined a significant increase of this bacterial family, reaching values of 30.66 %. However, when the CA15 strain was co-administrated with the antimycotic (CA15 + FCZ) a lower value (20.20 %) was achieved. Similar trend was displayed by the *Enterobacterales* genus, with lower relative frequency in CA15 (0.74 %) and Ctrl (1.12 %) samples than in those co-administrated with fluconazole (6.01 % Ctrl+FCZ and 3.58 % CA15 + FCZ). The *Subdoligranulum* genus also showed an increase in samples inoculated with CA15 compared to the Ctrl, with values of 2.27 % and 1.14 %, respectively. Similar trend was achieved when fluconazole was co-administrated, with values of 1.94 % (Ctrl+FCZ) and 2.19 % (CA15 + FCZ). Slight differences were found for the *Faecalibacterium* genus both in absence and in presence of fluconazole (Fig. 5). Compared to Ctrl, the *Oscillospiraceae* UCG-002 genus was affected by CA15 treatment, showing a 1 % reduction in values and representing the 4.02 % and 6.10 % of the total microbial population in samples with and without fluconazole administration, respectively.

Zooming on *Lachnospiraceae* family, including *Ruminococcus torques* and *Eubacterium halii* groups, they represent another important fraction in the colonic samples, with 15.24 % and 14.57 %, in Ctrl and CA15 samples, respectively, and values of 13.65 % and 12.74 %, in samples with antimycotic (Ctrl+FCZ and CA15 + FCZ, respectively). The same

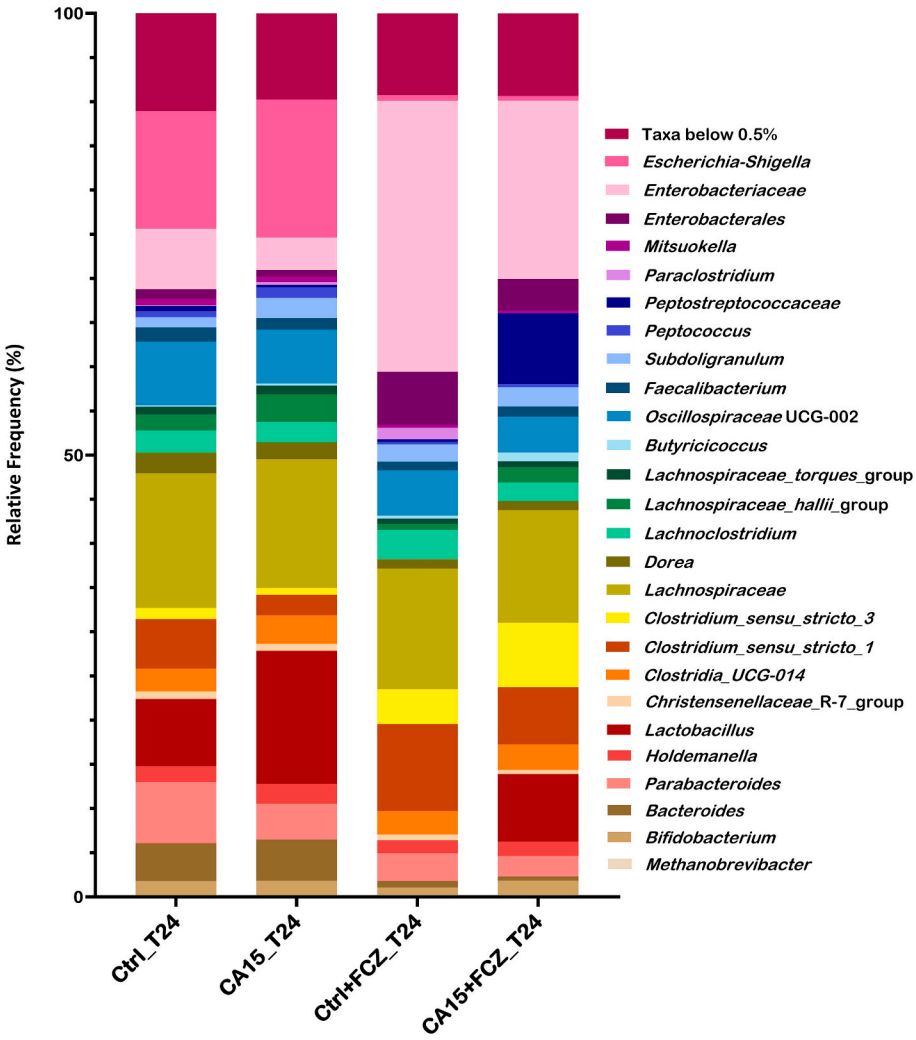

Fig. 5. Relative Frequency (%) of bacterial family and genus found on colonic samples with encapsulate probiotic L. *rhamnosus* CA15, under fasted condition, with and without antimycotic Fluconazole treatment.

trend was showed for *Dorea* genus with a lower value in samples with antimycotic. *Clostridium_sensu_ stricto_ 1* and *Clostridium_sensu_ stricto_ 3* genera were found reduced in CA15 compared to the Ctrl, instead *Clostridia_UCG-014* genus slightly increased. However, the fluconazole did not inhibit these genera, showing a reduction effect only for *Clostridium_sensu_ stricto_* 1 (6.47 %) compared to the Ctrl+FCZ (9.83 %). The *Lactobacillus* genus appeared to be influenced by the administration of the CA15, both with and without fluconazole. In detail, the *Lactobacillus* genus exhibited an abundance of 15.08 % in sample without the antimycotic, compared to 7.60 % in the Ctrl. In the fluconazole-treated samples, this genus reached an abundance of 7.67 %, compared to a value lower than 0.01 % in the control with fluconazole (Ctrl+FCZ). These findings highlight the role of the CA15 strain in the mitigation of antimycotic effect on *Lactobacillus* population. The *Parabacteroides* genus was negatively affected by the probiotic treatment, showing a decrease in sample with CA15 (4.06 %) compared to Ctrl (6.90 %), as well as in presence of fluconazole. The *Bacteroides* genus was significantly reduced by the antimycotic treatment, although no notable differences were observed when comparing the control and CA15 groups in either case. No significant variation was found on *Bifidobacterium* genus in CA15 (1.67 %) and Ctrl (1.64 %) samples, and lower values were found when fluconazole was co-administrated with CA15 strain (0.84 % and 1.61 %, respectively).

1.1. Metabolomic profile of colonic fraction from SHIME®

An objective comparison of lumen samples from SHIME® colonic fraction were analysed to determine VOCs, SCFAs and BCFAs profiles after 0, 2 and 24 h of incubation. Ninety-nine volatile metabolites were identified and classified in the following chemical classes: alcohols (11), aldehydes (9), carboxylic esters (16), carboxylic acids (5), hydrocarbons (18), phenols (2), indoles (3), ketones (6), terpenes (14) (Data not shown). Other fifteen compounds not belonging to the listed classes were identified (Hexane, 2,3,4-trimethyl-; Furfural; 2-n-Propyl-1-heptanol; Benzofuran, 2,3-dihydro-; 2-Decenal, (*Z*)-; p-Aminotoluene; . gamma.-Dodecalactone; Acetonitrile; Decane, 2,4-dimethyl-; 1,2-Benzenediol, o-(4-butylbenzoyl)-o'-(2-methylbenzoyl)-; Benzene, 1-ethyl-2,4-dimethyl-; Anethole; Dimethyl trisulfide; Ethylamine; Pyrazine, 2,6-dimethyl-).

The multivariate analysis of principal components (PCA) based on the coupled gas chromatography/mass spectrometry metabolomics data demonstrates how the different sampling time leads to a shift in VOC profiles after 24 h of colonic incubation (Fig. 6). In detail, the not supervised PCA explaining 54 % of variance, showed how the lumen sampled from colonic fraction after 24 h were plotted in the second and third quadrant, whereas the first two sampling times (0 and 2 h) were mostly plotted in the first and fourth quadrants. To evaluate the statistically significant differences in terms of VOCs among lumen samples after 24 h of colonic incubation, we computed a pairwise comparison combining results from fold change analysis and Wilcoxon rank-sum test. The volcano plot showed how the administration of L. *rhamnosus*

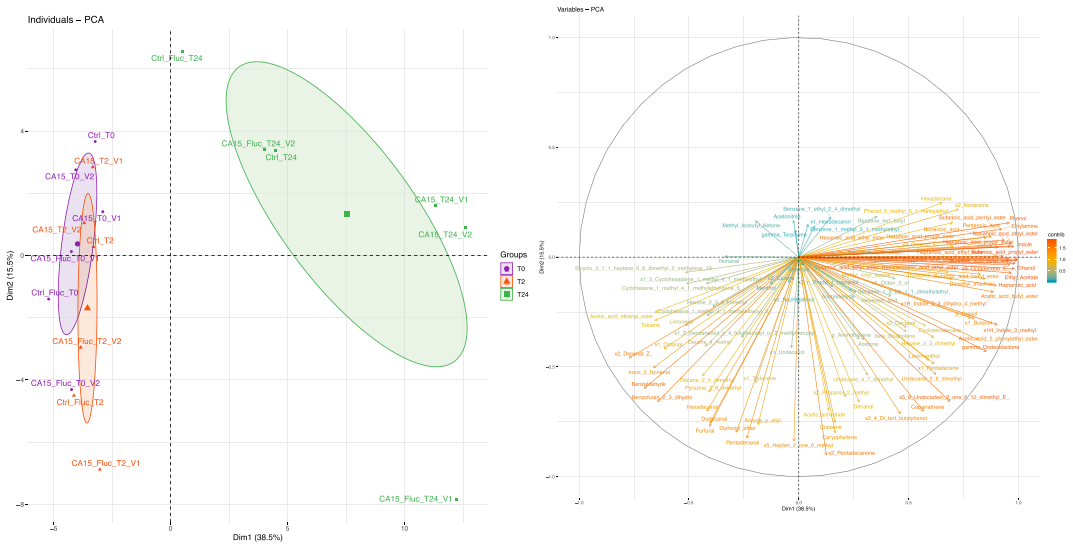

Fig. 6. Principal component analysis of VOCs in lumen samples from SHIME colonic fraction under fed condition with administration of encapsulated probiotic L. *rhamnosus* CA15 (CA15), probiotic *L. rhamnosus* CA15 with fluconazole (CA15_Fluc), control (Ctrl) and control with fluconazole (Ctrl_Fluc) after 0, 2 and 24 h of fermentation marked in violet, orange and green respectively. (For interpretation of the references to colour in this figure legend, the reader is referred to the web version of this article.)

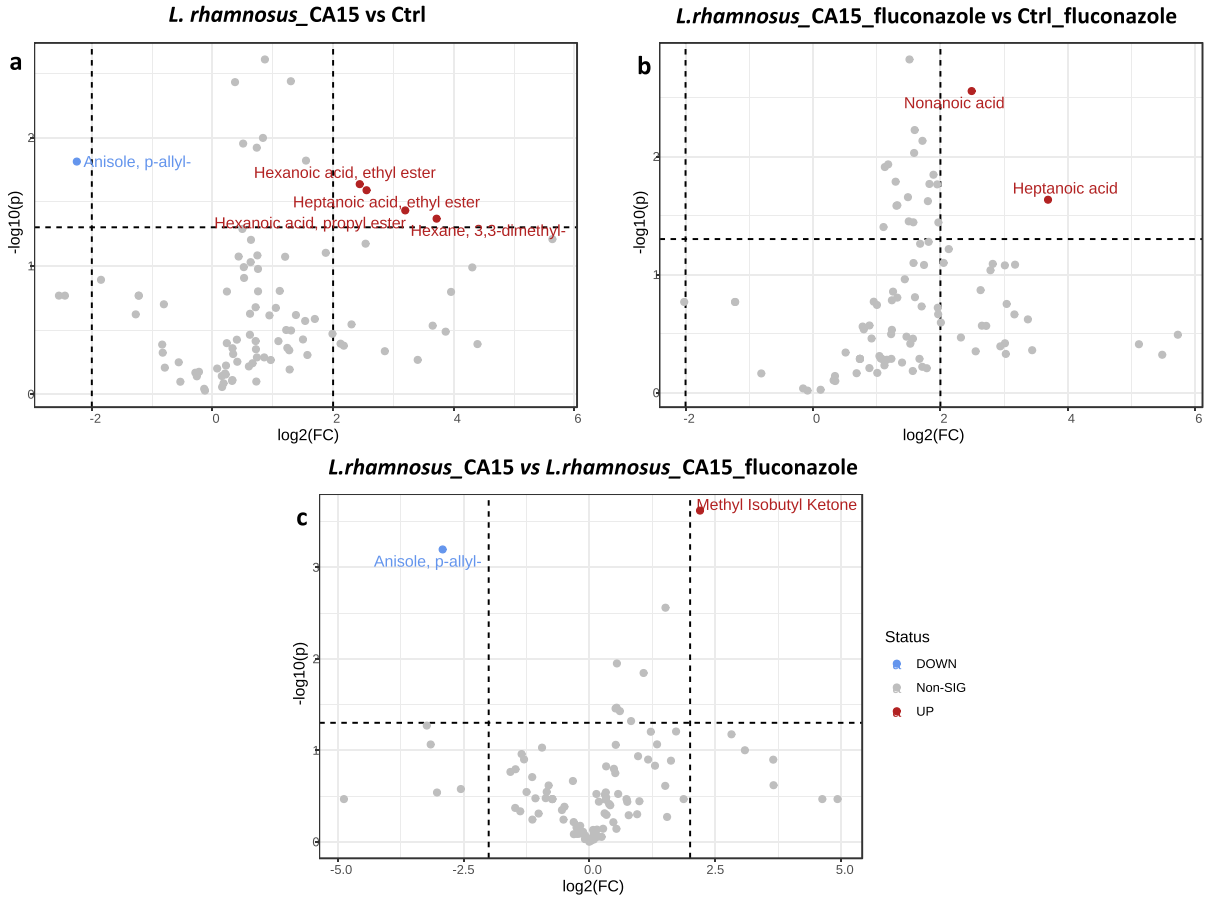

Fig. 7. Volcano plot of statistically significant VOC in duodenal lumen sample after 24 h of fermentation. Pairwise comparison of VOC in lumen samples after 24 h of fermentation by meaning of a non-parametric Wilcoxon rank-sum test ($p < 0.05$) combined with a fold change analysis (log2FC >2). Due to the group comparison direction, increased (up-red) and decreased (down-blue) VOC concentrations are relative to (a) probiotic *L. rhamnosus* CA15 to control; (b) probiotic *L. rhamnosus* CA15 with fluconazole to control with fluconazole. (For interpretation of the references to colour in this figure legend, the reader is referred to the web version of this article.)

CA15 with and without fluconazole increased the amount of medium fatty acids (heptanoic acid, nonanoic acid) and derivative esters (heptanoic acid ethyl ester, hexanoic acid ethyl ester and propyl ester) respectively (Fig. 7). The lonely administration of L. *rhamnosus* CA15 seemed to decrease the concentration of Anisole, p-allyl- (Estragole) and increase of methyl isobutyl ketone compared to probiotic administration with fluconazole.

In the simulated colon environment, the probiotic with or without fluconazole administration's effect on the microbial activity was assessed by evaluating the levels of SCFA and BCFA at different time points. As expected, statistically significant differences among sampling time were observed within each experimental theses after 24 of colonic incubation (Supplementary table 2). We than used the one-way analysis of variance (ANOVA) to determine whether there were any statistically significant differences between groups after 24 h of colonic incubation (Fig. 8). Acetic acid, propanoic acid and isobutyric acid were the most affected metabolites. Specifically, an increase ($p < 0.05$) was observed when L. *rhamnosus* was compared to control, and when compared to experimental theses with fluconazole (*L. rhamnosus* CA15_Fluconazole). No statistically significant differences were observed between CA15 and CA15 with fluconazole. Concerning the butanoic acid and isovaleric acid, any statistically significant differences were observed after L. *rhamnosus* CA15.

3.5. Correlation analysis of VOCs and microbial taxa

A linear Pearson correlation allowed us to trace a possible bridge connection between 16S selected taxa, and GC/MS statistically significant results, from both an untargeted and a targeted approaches resulting as VOCs and SCFAs, respectively (Fig. 9). Among cross correlated variables it is worth to be noticed how an increase of *Faecalibacterium* genus is positively correlated with almost all SCFAs. Apart for isovalerate, this is true for all the other measured SCFA plus nonanoic acid. On the contrary, isovalerate together with heptanoic acid is negatively correlated with *Paraclostridium* genus. Similarly, hexanoic acid propyl ester was negatively correlated with *Subdoligranulum*. Methyl isobutyl ketone is positively correlated with *Dorea*, *Mitsuokella* and *Christensenellaceae*_R-7_group. Finally, propanoic acid positively correlated with *Parabacteroides* and *Dorea*.

4. Discussion

In the present study a short-term experiment under both fasted and fed conditions was carried out to investigate the survival rate of the L. *rhamnosus* CA15 probiotic strain in the upper GIT using the SHIME® model. In addition, the survivability of the CA15 strain in presence of fluconazole under fasted condition was evaluated. Metagenetic and metabolomic profiles of colonic samples were analysed to provide an integrated view of microbial and metabolic modulation.

The results showed that the CA15 probiotic strain maintained high viability in both fasted and fed conditions, with a significant increase in the latter stages of the small intestine, especially under the fasted condition. This result indicates that the physiological state of the digestive system may influence both survival and persistence of probiotic strains, suggesting that the fasted state may represent a more favourable environment, possibly due to the reduced enzyme activity and faster transit time, which could reduce exposure to harmful factors. The use of the *in vitro* SHIME® model to study the upper intestinal fraction was introduced for the first time in a study conducted by Marzorati et al. (2015), who had demonstrated an improved survivability of the L. *rhamnosus* LGG and *Bifidobacterium lactis* BB12 strains under fasted condition. A similar outcome was observed in a subsequent study by Marzorati et al. (2021), testing the *Lactobacillus acidophilus* LA-14 strain. These findings support the hypothesis demonstrated in the present study, that, under fasting condition, the rate of gastric emptying and reduced enzymatic activity, can significantly improve the passage and delivery of the CA15 strain to the colon. In particular, the culture-dependent approach, used to assess the viability of the CA15 strain in both the stomach and the small intestine fraction, confirmed its capability to survive under both fed and fasted condition, with a value of 6 log CFU/mL and 7 log CFU/mL, respectively. In the colonic compartment, the reduction in the number of viable cells of the CA15 strain, as disclosed by the RT-qPCR analysis, could be due to environmental stressors such as anaerobiosis and nutrient depletion.

According to studies on the effectiveness of probiotic supplementation with antimycotics (Martinez et al., 2009; Vahedpoor et al., 2021), the combined use of fluconazole and probiotic treatment was also proposed in our study. We observed that the simultaneous administration of fluconazole did not negatively compromise the viability of the CA15 probiotic strain in both the stomach and small intestine fractions. However, it is important to consider the potential impact of antifungal treatment on the gut microbiota composition, as it can affect the diversity and balance of this microbial community (Yang, Wei, et al., 2024). It is well known that antimicrobials can impact the gut microbiota and antifungals have the potential to influence the balance of the gut microbial community (Maier et al., 2018). Although, several studies suggested that certain antifungal drugs, particularly imidazoles, may have direct antimicrobial activity against both bacterial pathogens and commensals of the gut, for antifungal triazoles, including fluconazole, antimicrobial activity against gut microbes has not been observed (Maier et al., 2018). Moreover, to date, no scientific studies in humans have been conducted to evaluate the effect of fluconazole on the colonic bacterial population, apart from its impact on *Candida* species. In this regard, Heng et al. (2021) examined the impact of fluconazole on the gut microbiota composition in mice. Their findings indicated that the gut microbial composition was significantly changed after fluconazole treatment. In particular, by studying the bacteriome, a significant increase in *Firmicutes* and *Proteobacteria*, along with a remarkable reduction in *Bacteroidetes*, *Deferribacteres*, *Patescibacteria*, and *Tenericutes* were revealed in mice receiving fluconazole treatment compared with the

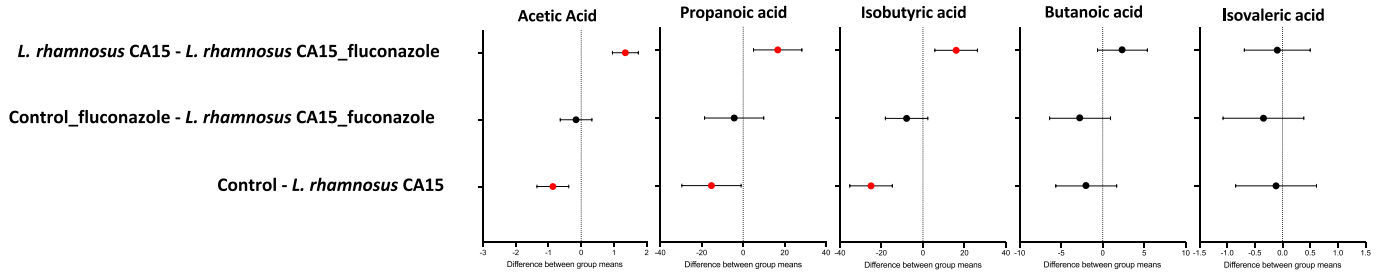

Fig. 8. Pairwise comparison of SCFAs (acetic acid, propanoic acid, isobutyric acid and butanoic acid) BCFA (isovaleric acid) showing differences between lumen sample from SHIME® colonic fraction after 24 h of fermentation according to direction of comparison. 95 % of confidence interval of differences between group were plotted and statistically significant differences (Anova one-way corrected by Tukey's test) were marked in red. (For interpretation of the references to colour in this figure legend, the reader is referred to the web version of this article.)

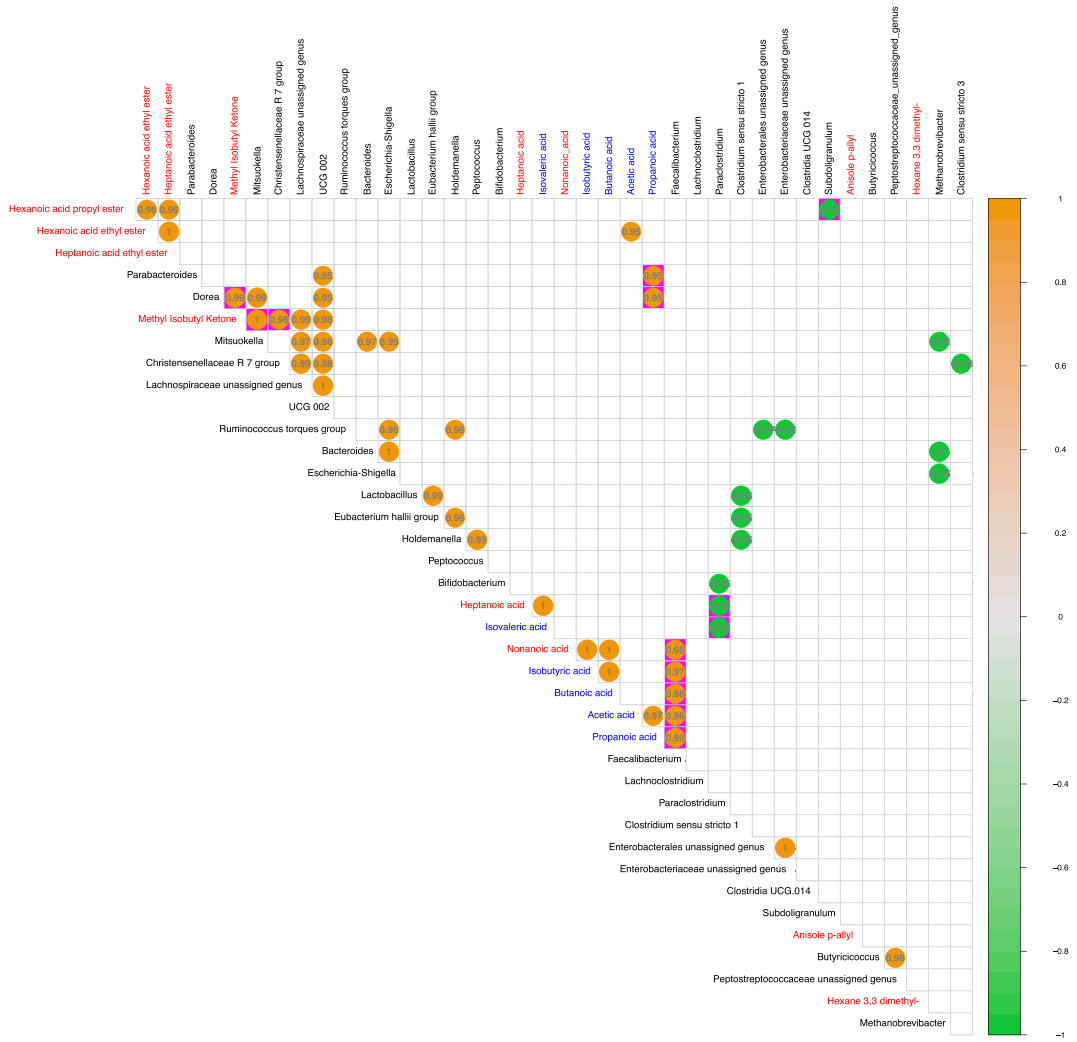

Fig. 9. VOC *versus* genus correlation. Pearson's correlation between statistically significant VOCs non-parametric Wilcoxon rank-sum test ($p < 0.05$) and selected bacterial genera. Black font is relative to taxa variables, whereas blue and red font characters refer to VOC (from GC–MS untargeted approach) or SCFA, respectively. Only statistically significant correlations (*p*-value <0.01) with an R value greater than 0.7 have been reported. Cross comparisons have been plotted as correlation values on a purple background. Negative and positive correlations have been indicated based on a scaled colour bar from green to orange. The size of the circles is proportional to the correlation value, both in case of a positive or negative correlation. (For interpretation of the references to colour in this figure legend, the reader is referred to the web version of this article.)

control group. According to that, in our study, fluconazole determined changes in the relative abundance of specific microbial groups. Particularly, we observed a reduction of *Firmicutes* and an increase of *Proteobacteria*. In addition, a decrease of *Dorea*, *Mitsuokella*, *Lactobacillus*, *Oscillospiraceae* UCG-002, and *Bifidobacterium* genera, as well as *Christensenellaceae*_R-7_group and *Eubacterium hallii* was recorded. Most of these genera are commensal gut microbiota, associated with health-promoting benefits which include the production of metabolites, such as short-chain fatty acids and vitamins, immune system development, and prevention of gut disorders (Krishnamurthy et al., 2023). On the contrary, the fluconazole seems to promote the relative abundance of *Enterobacteriaceae,* notoriously associated with inflammatory conditions, such as IBD, obesity, colorectal cancer, celiac disease, and antibiotic treatment as well as nosocomial infections with other microbes (Furuichi et al., 2024; Zeng et al., 2017). These findings provide additional insights into the effect of fluconazole treatment on the gut bacterial composition. However, it is interesting to note that the co-administration of the CA15 strain counteracts, in the colonic fraction, the changes induced by the antimycotic treatment. In particular, the CA15 strain co-administration reduced the relative abundance of *Enterobacteriaceae* and slightly increased the *Faecalibacterium*, which is capable of breaking down complex polysaccharides into monosaccharides which are further fermented into SCFAs (acetic acid, propanoic acid, butanoic acid and isobutyric acid) and medium-chain fatty acids (nonanoic acid), exerting beneficial microbial balance (Sharon et al., 2014; Hoeck et al., 2017). Since these metabolites play a recognized role in gut health, in the present study, their increase can be interpreted as a positive functional output of CA15 administration.

Evaluating the metabolome, the L. *rhamnosus* CA15 strain affected SCFAs and BCFAs and their derivative esters, which are known to exert several beneficial effects, such as energy source, regulation of glucose and lipid metabolisms, protective action against inflammation, neuroprotective activity, and regulation of the gut innate and adaptive immune responses (LeBlanc et al., 2017; Roopashree et al., 2021; Sam et al., 2021). In addition, we observed a decrease of methyl isobutyl ketone after fluconazole treatment. The elevated levels of this compound likely reflect a gut microbial imbalance, consistent with previous reported association in other conditions such as autism spectrum disorders, NAFLD/NASH, and Juvenile Idiopathic Arthritis (Vernocchi et al., 2023). The increase of nonanoic acid and heptanoic acid in CA15 samples, with and without fluconazole, compared to control, suggests a potential beneficial activity on intestinal epithelial immunological

barrier function (Wang et al., 2018).

A limitation of this study is the inability to fully capture the effective influence of the CA15 strain on the microbiota and metabolome of the large intestine. Indeed, further long experiment studies, focusing on the proximal and distal colon fractions, are planned. These will account for the necessary stabilization phases of the instrument in order to simulate an *in vivo* condition that would allow to highlight the effects on the intestinal microbiota and metabolome, following prolonged probiotic administration.

5. Conclusion

In conclusion, the use of a dynamic *in vitro* system, such as the SHIME® model, allowed a comprehensive understanding of the delivery and bioavailability of the probiotic L. *rhamnosus* CA15 strain in the upper gastrointestinal tract and subsequently in the colonic fraction. In addition, the application of molecular methods coupled with strain-specific primers allowed a more sophisticated qualitative-quantitative detection of the L. *rhamnosus* CA15 strain, in the colonic environment. The present study has demonstrated the effect of fluconazole treatment on the gut bacterial composition, which was partially mitigated by the CA15 strain co-administration, suggesting its promising use during the antimycotic treatment.

CRediT authorship contribution statement

Amanda Vaccalluzzo: Writing – review & editing, Writing – original draft, Methodology, Formal analysis, Data curation. **Giuseppe Celano:** Writing – review & editing, Formal analysis, Data curation. **Francesco Maria Calabrese:** Formal analysis, Data curation. **Alessandra Pino:** Writing – review & editing, Methodology. **Cinzia Caggia:** Writing – review & editing, Conceptualization. **Maria De Angelis:** Writing – review & editing, Conceptualization. **Cinzia Lucia Randazzo:** Writing – review & editing, Supervision, Methodology, Conceptualization.

Ethical statement

Faecal samples of the donor were collected during the clinical trial approved by local Ethical Committee (registration number 163/2022/PO).

Declaration of competing interest

The authors declare that they have no known competing financial interests or personal relationships that could have appeared to influence the work reported in this paper.

Appendix A. Supplementary data

Supplementary data to this article can be found online at https://doi.org/10.1016/j.foodres.2025.117757.

Data availability

Data will be made available on request.

References

Dornelas-Figueira, L. M., Ricomini Filho, A. P., Junges, R., Åmdal, H. A., Cury, A. A. D. B., & Petersen, F. C. (2023). In vitro impact of fluconazole on Oral microbial communities, bacterial growth, and biofilm formation. *Antibiotics, 12*(9), 1433. https://doi.org/10.3390/antibiotics12091433

FAO/WHO. (2002). Guidelines for the evaluation of probiotics in food. *Report of a Joint FAO/WHO Working Group. FAO/WHO*, 1–10. http://www.fao.org/3/a-a0512e.pdf.

Furuichi, M., Kawaguchi, T., Pust, M. M., Yasuma-Mitobe, K., Plichta, D. R., Hasegawa, N., … Honda, K. (2024). Commensal consortia decolonize Enterobacteriaceae via ecological control. *Nature, 633*(8031), 878–886. https://doi.org/10.1038/s41586-024-07960-6

Han, J., McClements, D. J., Liu, X., & Liu, F. (2024). Oral delivery of probiotics using single-cell encapsulation. *Comprehensive Reviews in Food Science and Food Safety, 23*(3), Article e13322. https://doi.org/10.1111/1541-4337.13322

Han, S., Lu, Y., Xie, J., Fei, Y., Zheng, G., Wang, Z., & Li, L. (2021). Probiotic gastrointestinal transit and colonization after oral administration: A long journey. *Frontiers in Cellular and Infection Microbiology, 11*, Article 609722. https://doi.org/10.3389/fcimb.2021.609722

Heng, X., Jiang, Y., & Chu, W. (2021). Influence of fluconazole administration on gut microbiome, intestinal barrier, and immune response in mice. *Antimicrobial Agents and Chemotherapy, 65*(6), 10–1128. https://doi.org/10.1128/aac.02552-20

Hoek, M. J. V., & Merks, R. M. (2017). Emergence of microbial diversity due to cross-feeding interactions in a spatial model of gut microbial metabolism. *BMC Systems Biology, 11*, 1–18. https://doi.org/10.1186/s12918-017-0430-4

Jannin, V., Duysburgh, C., Gonzalez, V., Govaert, M., Agisson, M., Marzorati, M., & Madit, N. (2023). In vitro evaluation of the gastrointestinal delivery of acid-sensitive pancrelipase in a next generation enteric capsule using an exocrine pancreatic insufficiency disease model. *International Journal of Pharmaceutics, 630*, Article 122441. https://doi.org/10.1016/j.ijpharm.2022.122441

Klindworth, A., Pruesse, E., Schweer, T., Peplies, J., Quast, C., Horn, M., & Glöckner, F. O. (2013). Evaluation of general 16S ribosomal RNA gene PCR primers for classical and next-generation sequencing-based diversity studies. *Nucleic Acids Research, 41*(1), e1. https://doi.org/10.1093/nar/gks808

Krishnamurthy, H. K., Pereira, M., Bosco, J., George, J., Jayaraman, V., Krishna, K., … Rajasekaran, J. J. (2023). Gut commensals and their metabolites in health and disease. *Frontiers in Microbiology, 14*, Article 1244293. https://doi.org/10.3389/fmicb.2023.1244293

Lauriero, G., Abbad, L., Vacca, M., Celano, G., Chemouny, J. M., Calasso, M., … Monteiro, R. C. (2021). Fecal microbiota transplantation modulates renal phenotype in the humanized mouse model of IgA nephropathy. *Frontiers in Immunology, 12*, Article 694787. https://doi.org/10.3389/fimmu.2021.694787

LeBlanc, J. G., Chain, F., Martín, R., Bermúdez-Humarán, L. G., Courau, S., & Langella, P. (2017). Beneficial effects on host energy metabolism of short-chain fatty acids and vitamins produced by commensal and probiotic bacteria. *Microbial Cell Factories, 16*, 1–10. https://doi.org/10.1186/s12934-017-0691-z

Li, C., Yu, W., Wu, P., & Chen, X. D. (2020). Current in vitro digestion systems for understanding food digestion in human upper gastrointestinal tract. *Trends in Food Science & Technology, 96*, 114–126. https://doi.org/10.1016/j.tifs.2019.12.015

Lionetti, E., Dominijanni, V., Iasevoli, M., Cimadamore, E., Acquaviva, I., Gatti, S., … Catassi, C. (2023). Effects of the supplementation with a multispecies probiotic on clinical and laboratory recovery of children with newly diagnosed celiac disease: A randomized, placebo-controlled trial. *Digestive and Liver Disease, 55*(10), 1328–1337. https://doi.org/10.1016/j.dld.2023.04.021

Maier, L., Pruteanu, M., Kuhn, M., Zeller, G., Telzerow, A., Anderson, E. E., … Typas, A. (2018). Extensive impact of non-antibiotic drugs on human gut Bacteria. *Nature, 555*, 623–628. https://doi.org/10.1038/nature25979

Martin, M. V. (1999). The use of fluconazole and itraconazole in the treatment of Candida albicans infections: A review. *Journal of Antimicrobial Chemotherapy, 44*(4), 429–437. https://doi.org/10.1093/jac/44.4.429

Martinez, R. C. R., Franceschini, S. A., Patta, M. C., Quintana, S. M., Candido, R. C., Ferreira, J. C., … Reid, G. (2009). Improved treatment of vulvovaginal candidiasis with fluconazole plus probiotic Lactobacillus rhamnosus GR-1 and Lactobacillus reuteri RC-14. *Letters in Applied Microbiology, 48*(3), 269–274. https://doi.org/10.1111/j.1472-765X.2008.02477.x

Marzorati, M. (2018). SHIME®: An advanced in vitro technology platform for studying the mode-of-action of probiotics in the gastrointestinal tract. *International Journal on Nutraceuticals, Functional Foods and Novel Foods*. https://doi.org/10.17470/NF-018-1023-4

Marzorati, M., Calatayud, M., Rotsaert, C., Van Mele, M., Duysburgh, C., Durkee, S., … Bellamine, A. (2021). Comparison of protection and release behavior of different capsule polymer combinations based on L. acidophilus survivability and function and caffeine release. *International Journal of Pharmaceutics, 607*, Article 120977. https://doi.org/10.1016/j.ijpharm.2021.120977

Marzorati, M., Possemiers, S., Verhelst, A., Cadé, D., Madit, N., & Van de Wiele, T. (2015). A novel hypromellose capsule, with acid resistance properties, permits the targeted delivery of acid-sensitive products to the intestine. *LWT- Food Science and Technology, 60*(1), 544–551. https://doi.org/10.1016/j.lwt.2014.08.040

Minelli, E. B., & Benini, A. (2008). Relationship between number of bacteria and their probiotic effects. *Microbial Ecology in Health and Disease, 20*(4), 180–183. https://doi.org/10.1080/08910600802408095

Molly, K., Vande Woestyne, M., & Verstraete, W. (1993). Development of a 5-step multi-chamber reactor as a simulation of the human intestinal microbial ecosystem. *Applied Microbiology and Biotechnology, 39*, 254–258. https://doi.org/10.1007/978-3-319-16104-4_27

Pappas, P. G., Kauffman, C. A., Andes, D. R., Clancy, C. J., Marr, K. A., Ostrosky-Zeichner, L., … Sobel, J. D. (2016). Clinical practice guideline for the management of candidiasis: 2016 update by the Infectious Diseases Society of America. *Clinical Infectious Diseases, 62*(4), e1–e50. https://doi.org/10.1093/cid/civ933

Pino, A., Vaccalluzzo, A., Caggia, C., Balzaretti, S., Vanella, L., Sorrenti, V., & Randazzo, C. L. (2022). Lacticaseibacillus rhamnosus CA15 (DSM 33960) as a candidate probiotic strain for human health. *Nutrients, 14*(22), 4902. https://doi.org/10.3390/nu14224902

Rinninella, E., Raoul, P., Cintoni, M., Franceschi, F., Miggiano, G. A. D., Gasbarrini, A., & Mele, M. C. (2019). What is the healthy gut microbiota composition? A changing

ecosystem across age, environment, diet, and diseases. *Microorganisms, 7*(1), 14. https://doi.org/10.3390/microorganisms7010014

Roopashree, P. G., Shetty, S. S., & Kumari, N. S. (2021). Effect of medium chain fatty acid in human health and disease. *Journal of Functional Foods, 87*, Article 104724. https://doi.org/10.1016/j.jff.2021.104724

Sam, Q. H., Ling, H., Yew, W. S., Tan, Z., Ravikumar, S., Chang, M. W., & Chai, L. Y. A. (2021). The divergent immunomodulatory effects of short chain fatty acids and medium chain fatty acids. *International Journal of Molecular Sciences, 22*(12), 6453. https://doi.org/10.3390/ijms22126453

Sharon, G., Garg, N., Debelius, J., Knight, R., Dorrestein, P. C., & Mazmanian, S. K. (2014). Specialized metabolites from the microbiome in health and disease. *Cell Metabolism, 20*(5), 719–730. https://doi.org/10.1016/j.cmet.2014.10.016

U.S. Food & Drug Administration (FDA). (2022). *Fluconazole label information. Drugs@FDA*.

Vaccalluzzo, A., Celano, G., Pino, A., Calabrese, F. M., Foti, P., Caggia, C., & Randazzo, C. L. (2022). Metagenetic and volatilomic approches to elicidate the effect of *Lactiplantibacillus plantarum* starter cultures on Sicilian table olives. *Frontiers in Microbiology, 12*, 771636. https://doi.org/10.3389/fmicb.2021.771636

Vahedpoor, Z., Abastabar, M., Sehat, M., Talebian, P., Fini, T. F., Dastanpour, Z., … Nazeri, M. (2021). Vaginal and oral use of probiotics as adjunctive therapy to fluconazole in patients with vulvovaginal candidiasis: A clinical trial on Iranian women. *Current Medical Mycology, 7*(3), 36. https://doi.org/10.18502/cmm.7.3.7803

Van de Wiele, T., Van den Abbeele, P., Ossieur, W., Possemiers, S., Marzorati, M. (2015). The simulator of the human intestinal microbial ecosystem (SHIME®). In: Verhoeckx K, Cotter P, López-Expósito I, Kleiveland C, Lea T, Mackie A, Requena T, Swiatecka D, Wichers H, editors. The impact of food bioactives on health: In vitro and ex vivo models [internet]. Cham (CH): Springer; 2015. Chapter 27. PMID: 29787058.

Van den Abbeele, P., Taminiau, B., Pinheiro, I., Duysburgh, C., Jacobs, H., Pijls, L., & Marzorati, M. (2018). Arabinoxylo-oligosaccharides and inulin impact inter-individual variation on microbial metabolism and composition, which immunomodulates human cells. *Journal of Agricultural and Food Chemistry, 66*(5), 1121–1130. https://doi.org/10.1021/acs.jafc.7b04611

Vernocchi, P., Marangelo, C., Guerrera, S., Del Chierico, F., Guarrasi, V., Gardini, S., … Putignani, L. (2023). Gut microbiota functional profiling in autism spectrum disorders: Bacterial VOCs and related metabolic pathways acting as disease biomarkers and predictors. *Frontiers in Microbiology, 14*, Article 1287350. https://doi.org/10.3389/fmicb.2023.1287350

Vitellio, P., Celano, G., Bonfrate, L., Gobbetti, M., Portincasa, P., & De Angelis, M. (2019). Effects of Bifidobacterium longum and Lactobacillus rhamnosus on gut microbiota in patients with lactose intolerance and persisting functional gastrointestinal symptoms: A randomised, double-blind, cross-over study. *Nutrients, 11*(4), 886. https://doi.org/10.3390/nu11040886

Wang, J., Huang, N., Xiong, J., Wei, H., Jiang, S., & Peng, J. (2018). Caprylic acid and nonanoic acid upregulate endogenous host defense peptides to enhance intestinal epithelial immunological barrier function via histone deacetylase inhibition. *International Immunopharmacology, 65*, 303–311. https://doi.org/10.1016/j.intimp.2018.10.022

Wang, Z. D., Zhang, W., & Liang, T. X. (2025). Advancements in Oral delivery Systems for Probiotics Based on polysaccharides. *Polymers, 17*(2), 144. https://doi.org/10.3390/polym17020144

Wendel, U. (2022). Assessing viability and stress tolerance of probiotics—A review. *Frontiers in Microbiology, 12*, Article 818468. https://doi.org/10.3389/fmicb.2021.818468

Yang, S., Qiao, J., Zhang, M., Kwok, L. Y., Matijašić, B. B., Zhang, H., & Zhang, W. (2024). Prevention and treatment of antibiotics-associated adverse effects through the use of probiotics: A review. *Journal of Advanced Research*. https://doi.org/10.1016/j.jare.2024.06.006

Yang, S., Wei, S., Wu, Y., Fang, Y., Deng, Z., Xu, J., & Zhang, H. (2024). Encapsulation techniques, action mechanisms, and evaluation models of probiotics: Recent advances and future prospects. *Food Frontiers, 5*(3), 1212–1239. https://doi.org/10.1002/fft2.374

Zeng, M. Y., Inohara, N., & Nunez, G. (2017). Mechanisms of inflammation-driven bacterial dysbiosis in the gut. *Mucosal Immunology, 10*, 18–26. https://doi.org/10.1038/mi.2016.75